High resolution TEM of chondritic carbonaceous matter: Metamorphic evolution and heterogeneity

Corentin Le Guillou, Jean-Noel Rouzaud, Lydie Bonal, Eric Quirico, Sylvie Derenne, Laurent Remusat

The Meteoritical Society

Meteoritics & Planetary Science 47, Nr 3, 345–362 (2012)
doi: 10.1111/j.1945-5100.2012.01336.x

High resolution TEM of chondritic carbonaceous matter: Metamorphic evolution and heterogeneity

Corentin LE GUILLOU[1*], Jean-Noël ROUZAUD[1], Lydie BONAL[2], Eric QUIRICO[2], Sylvie DERENNE[3], and Laurent REMUSAT[4]

[1]Laboratoire de Géologie de l'Ecole Normale Supérieure, UMR 8538 CNRS-ENS, Paris, France
[2]Université Joseph Fourier, CNRS/INSU, Laboratoire de Planétologie de Grenoble UMR 5109, Bâtiment D de Physique, BP 53, 38041 Grenoble Cedex 9, France
[3]BioEMCo, UMR CNRS/UPMC 7618, Paris, France
[4]Laboratoire de Minéralogie et Cosmochimie du Muséum, UMR CNRS 7202, Museum National d'Histoire Naturelle, CP52, 57 rue Cuvier, 75231 Paris Cedex 05, France
[*]Corresponding author. E-mail: corentin.san@gmail.com

(Received 07 July 2010; revision accepted 13 January 2012)

Abstract–The insoluble carbonaceous matter from 12 chondrites (CI, CM, CO, CV, EH, and UOC), was characterized by high resolution transmission electron microscopy (HRTEM). Besides ubiquitous nanoglobules, the insoluble organic matter from petrologic type 1 and 2 chondrites and Semarkona (LL 3.0) is composed of a highly disordered polyaromatic component. No structural differences were observed between these IOMs, in agreement with the limited thermal metamorphism they all experienced. In chondrites of petrologic type >3.0, the evolution of the IOM is controlled by the extent of thermal metamorphism. The polyaromatic layers, shorter than 1 nm in petrologic type ≤3.0 chondrites, grow up to sizes between 5 and 10 nm in petrologic type >3.6 chondrites, contributing to the increase of the degree of structural order. In addition, we find rare, but ubiquitous onion-like carbons, which may be the product of nanodiamond graphitization. The insoluble carbonaceous matter of the enstatite chondrite Sahara 97096 (EH 3) is different from the other meteorites studied here. It is more heterogeneous and displays a high abundance of graphitized particles. This may be the result of a mixture between (1) the disordered carbon located in the matrix, and (2) catalytic graphitized phases associated with metal, potentially originating from partial melting events. The structural and nanostructural evolution are similar in all IOMs. This suggests that the structure of the accreted precursors and the parent body conditions of their secondary thermal modifications (temperature, duration, and pressure) were similar. The limited degree of organization of the most metamorphosed IOMs compared with terrestrial rocks submitted to similar temperature suggests that the conditions are not favorable to graphitization processes, due to the chemical nature of the precursor or the lack of confinement pressure.

INTRODUCTION

Chondrites of petrologic type ≤3.0 are among the most pristine rocks of the solar system. They contain up to several weight percents of organic matter (Alexander et al. 2007), present as soluble (Pizzarello et al. 2006; Glavin et al. 2011) and insoluble compounds, the latter being the most abundant. Insoluble acid residues mainly occur as a mixture of fluffy material or as nanoglobules (Garvie and Buseck 2004; Derenne et al. 2005; Nakamura-Messenger et al. 2006). Minor carbonaceous crystalline forms such as nanodiamonds (Lewis et al. 1987; Huss and Lewis 1994, 1995; Daulton et al. 1996), graphite (Amari et al. 1990; Mostefaoui et al. 2000, 2005; Croat et al. 2004), or carbides (Christoffersen and Buseck 1983; Zolensky et al. 1989; Krot et al. 1997;

Daulton et al. 2002) are also present in the acid residues.

Nanodiamonds and organic matter (IOM) may initially originate from interstellar and/or nebular processes (Robert and Epstein 1982; Lewis et al. 1987; Huss and Lewis 1994a; Alexander et al. 1998, 2007; Guillois et al. 1999; Duley and Grishko 2001; Dai et al. 2002; Van Kerckhoven et al. 2002; Remusat et al. 2006, 2009). They later experienced postaccretion processes, such as aqueous alteration and/or thermal metamorphism in the meteorite parent body.

In addition to the main bulk insoluble organic matter (IOM), rare forms of carbonaceous matter have also been discovered by high resolution transmission electron microscopy (HRTEM), including onion-like carbons and soots in Allende (CV_{Ox}, Harris et al. 2000), carbon-coated sulfides and iron-carbides in Allende, Murchison (CM), Acfer 094 (ungrouped), Allan Hills 77307 (CO), and Meteorite Hills 00426 (CR) (Brearley 1999, 2002, 2008; Abreu and Brearley 2010; Harris et al. 2000). All of these carbon forms display various structures at the nanometer scale and could originate from multiple processes and locations (interstellar, nebular, and asteroidal events).

In terms of structural organization degree, HRTEM has shown that most of the IOM in the pristine chondrites Orgueil (CI), Murchison, Tagish Lake (ungrouped), and Acfer 094 is not strictly amorphous, but rather exhibits some local organization at the nanometer scale. It is made of randomly distributed stacks of polyaromatic units of one to four cycles, linked together by short aliphatic chains and ether bridges (Sephton et al. 1998; Brearley 2002, 2008; Derenne et al. 2005; Rouzaud et al. 2005; Remusat et al. 2006).

Aqueous alteration increases from petrologic type 3 to 1 and was inferred to chemically modify the IOM. For instance, Cody and Alexander (2005) showed that the aliphatic to aromatic ratio was higher in CR2 than in CI1 chondrites, and Alexander et al. (2007) showed that CR2 had higher hydrogen on carbon (H/C) ratio than CI and CM2. It cannot be excluded that the initial composition of the OM was different, but these trends are correlated to aqueous alteration degrees. However, Raman spectroscopy, sensitive to some extent to the chemical composition of the carbonaceous material, does not reveal differences among CI, CM, and CR chondrites (Busemann et al. 2007). This apparent discrepancy may imply that these chemical changes do not affect the structure, e.g., mostly the size of the aromatic layers. Petrologic types ranging from 3.0 to 3.9 are defined to describe the increasing degree of parent body thermal metamorphism which modifies the carbonaceous materials as well. Indeed, with increasing temperature, their aromaticity increases and hydrogen and nitrogen are progressively released from the molecules. Raman spectroscopy is an efficient tool to evaluate the structural organization degree of the IOM, as it is sensitive to its progressive chemical evolution and polyaromatic layer growth. Spectral parameters of the carbonaceous matter Raman bands correlate with the metamorphic degree of type 3 chondrites, as defined by independent metamorphic tracers (Quirico et al. 2003, 2005a, 2009; Bonal et al. 2006, 2007; Busemann et al. 2007). For the temperature range involved in parent body metamorphism of type ≤3 chondrites, the modifications of the IOM correspond mostly to a carbonization process, where hydrogen and nitrogen are progressively lost. However, to a more limited extent, for petrologic type >3, it also corresponds to a structural improvement (sometimes called "graphitization process" even if graphite is not obtained), consisting in the growth and improvement of stacking of the polyaromatic layers, eventually leading to the development of the triperiodic order (AB stacking, i.e., strictly speaking, graphitization). Carbonization and graphitization are two processes extensively studied on terrestrial materials, such as laboratory pyrolyzed synthetic organic matter (Bény-Bassez and Rouzaud 1985; Beyssac et al. 2003), or natural organic matter (coals, kerogens, etc.) submitted to increasing metamorphism (Jehlicka and Rouzaud 1990; Wopenka and Pasteris 1993; Beyssac et al. 2002; Quirico et al. 2005b). Those studies show that the size of the polyaromatic layers and their mutual orientation in space, i.e., their nanostructure, as observed by HRTEM, are a fingerprint of the physical conditions of their formation and of the chemical nature of their precursors.

A few HRTEM studies describe the carbon organization of these thermally modified chondritic IOM at the nanometer-scale (Smith and Buseck 1981; Lumpkin 1986; Harris et al. 2000; Rouzaud et al. 2005; Remusat et al. 2008). Most of these studies focused on a limited set of objects. Here, we undertake a comparative HRTEM study of 12 acid residues from chondrites of various chemical groups and of petrologic types from 1 to 3.6. We focus on the structure and nanostructure of the IOM and assess their similarities and differences. The main objectives of the present work are to better (1) understand the evolution of the carbonaceous materials with metamorphism on the parent body, and (2) constrain the physical conditions of the thermal history of primitive chondrites.

MATERIAL AND METHODS

Chemical Separation of the IOMs

Table 1 lists the studied samples and their suppliers. The sample of Tagish Lake (originally prepared by M. Zolensky) is a pristine one which was recovered before the spring thaw of Tagish Lake submerged the

Table 1. Compilation of the different carbon forms observed in addition to the fluffy OM in the present work and reported in the literature, together with the elementary composition of the bulk IOM (from Alexander et al. 2007).

	Group	Globules	Graphitized particles	Onion-like carbon	Mean fringe length (nm)	H/C (at.)	O/C (at.)	N/C (at.)	S/C (at.)
CC									
Tagish Lake (a)	Ungrouped	✔ (1)			< 0.6				
Orgueil (b)	CI	✔ (2)		✔ (2)	< 0.6	67.3 ± 1.7	18.1 ± 0.2	3.5 ± 0.01	2.8 ± 1.4
Murchison (b)	CM 2	✔ (1)			< 0.6	58.8 ± 1.6	18.3 ± 0.3	3.27 ± 0.03	1.8 ± 1.2
Kaba (c)	CVox 3.1				2	31.1	30.3	1.23	n.m.
Leoville (c)	CVred 3.1–3.4				2	16.4 ± 0.2	9 ± 0.1	1.15 ± 0.08	n.m.
Mokoia (c)	CVox 3.6		✔		7.5	20.4 ± 0.3	13.2 ± 0.2	0.88 ± 0.01	n.m.
Allende (c)	CVox > 3.6		✔	✔ (6)	7.5	17.4 ± 1.0	12.5 ± 0.5	0.48 ± 0.03	n.m.
Ornans (c)	CO > 3.6				7.5				
Kainsaz (b)	CO 3.6	✔	✔ (3)	✔ (3)	7.5	16.3	11.9	0.6	n.m.
UOCs									
Semarkona (d)	3	✔	✔ (4)		< 0.6	47.6	28.9	1.49	7.4
Tieschitz (c)	3.6				7.5	16 ± 0.4	13.6 ± 0.4	1.01 ± 0.01	n.m.
EH									
Sahara 97096 (e)	3.1–3.4	✔	✔	✔	n.m.	0.31	n.m.	0.005	n.m.

The letter associated with the meteorite name indicates the person who performed the chemical extraction: (a) S. Pizzarello; (b) L. Remusat; (c) L. Bonal; (d) Yang and Epstein (1983); (e) S. Derenne. The tick mark indicates that the associated component has been observed in the residue during the present work, and the associated number relates to articles where those components have already been described: (1) Garvie and Buseck (2004); (2) Garvie and Buseck (2006); (3) Remusat et al. (2008); (4) Brearley (1990); (5) Brearley (2002); (6) Brearley (1999) n.m. = not measured.

sample into lake water (Zolensky et al. 2002). It may belong to the carbonate-poor lithology, the carbonate-rich lithology, or both. The chemical separation procedure has been previously described in detail (e.g., Yang and Epstein 1983; Gardinier et al. 2000). In brief, samples are crushed and subjected to extractions in water, acetone, and dichloromethane/methanol to extract the soluble organic components. The solid residues are then subjected to several HF/HCl treatments at room temperature. The final residues contain organic matter, as well as oxides and other insoluble inorganic phases.

Transmission Electron Microscopy

Transmission electron microscopy images were acquired on a Philips CM20 and a JEOL 2011 operating at 200 kV and using LaB_6 filament. The acid residue powders were dispersed in ethanol on TEM grids covered by lacey amorphous carbon films. All HRTEM images were taken from the thinnest ($\ll$ 20 nm) edges of the particles, above holes of the carbon film. The structural organization was directly imaged by using the ''high resolution'' mode (300–600 kx magnification). The smallest observable spacing in fringes mode is about 0.144 nm, due to theoretical microscope limitation, such as the aberration of sphericity. In the usual conditions of the Scherzer optimum, each fringe represents the profile of a polyaromatic layer.

Image analyses were conducted in a similar way as described by Derenne et al. (2005) and Remusat et al. (2008). In brief, quantitative structural and microtextural data are obtained after skeletonization of selected HRTEM images (Rouzaud and Clinard 2002). Pixel images of 1024 × 1024 with a resolution of 4000 ppi are produced, each pixel corresponding to 0.1725 nm. The image is processed by specific software that reduces the noise background by filtration in the Fourier transform domain. After selecting a threshold, a binary image is obtained and represents a skeleton of carbon layers profile. This skeleton is further analyzed with several criteria taken into account (1) all fringes shorter than an aromatic ring (i.e., 0.246 nm) have no physical sense and are eliminated; (2) the C–C bond being 0.142 nm, a fringe crossed by segments smaller than this value are considered as rectilinear; (3) two fringes spaced by more than 0.7 nm are considered as nonstacked layers as Van der Waals interactions between graphene layers are supposed to be negligible at this distance. Using this method, the length of all the fringes (L, i.e., the extent of the aromatic layers), was individually measured, by considering that a layer could be curved until a maximum distortion ratio arbitrarily fixed at 40%. As it is classically done with X-ray diffraction, coherent

domains are defined by the parts of the polyaromatic planes that are involved in the stacking of parallel planes (within a 15° margin). They are characterized by their diameter L_a and height L_c along with the number N of stacked layers and interlayer spacing d (Galvez et al. 2002; Rouzaud and Clinard 2002).

Terminology

Between strictly crystalline and amorphous material, carbonaceous materials display a wide range of intermediate states called "disordered carbons." They are characterized by a multiscale organization (structure, nanostructure) from the subnanometer to micrometer scale. The "structure" corresponds to the organization at the atomic scale of the carbon atoms within the polyaromatic layers. Carbonization and graphitization processes induce modifications of the size, curvature degree, stacking number, and structural defects (pentagonal instead of hexagonal carbon cycles for instance) of the polyaromatic layers. Turbostratic carbons consist of polyaromatic units stacked in parallel, but which have slipped out of alignment. Periodicity in the third dimension (c-axis) is therefore absent in turbostratic carbon. Due to the increase of Van der Waals forces between progressively more planar parallel polyaromatic layers, they tend to stack to form coherent domains, called "Basic Structural Units" (BSUs) (Oberlin 1989). The spatial arrangement of these BSUs, from the nanometer to the micrometer scale, gives rise to various "nanostructures" (lamellar, porous, concentric, fibrous, and so on) obtained from different precursors and conditions of formation. In the case of IOM, these nanostructures can be microporous (pore diameter < 2 nm), mesoporous (pore diameter between 2 and 50 nm), or macroporous (pore diameter > 50 nm), lamellar (made of parallel BSUs), or concentric (concentric orientation of the BSUs). The multiscale organization of both natural and anthropogenic carbonaceous materials is the fingerprint of both their precursors and their conditions of formation (Oberlin 1989; Rouzaud et al. 2005).

RESULTS

The TEM observations of the acid insoluble residues from the studied chondrites reveal the presence of three main components (Fig. 1a, Table 1):

1. Insoluble organic matter (IOM; C, H, O, N, and S bearing phases).
   - Highly disordered material, the most abundant component, was named "fluffy" by Garvie and Buseck (2006). We keep the terminology "fluffy organic matter (OM)" here.
   - Nanoglobules, detected in most samples. Their structure and morphologies have been previously described (Nakamura et al. 2001; Garvie and Buseck 2004, 2006) and are not the focus of this particular study.
2. Inorganic carbon phases (carbon bearing phases, but H is supposedly absent).
   - Graphitized carbons, close to perfectly crystalline graphite.
   - Onion-like carbons.
   - Nanodiamonds, carbides.
3. Other mineral phases, such as sulfides or oxides.

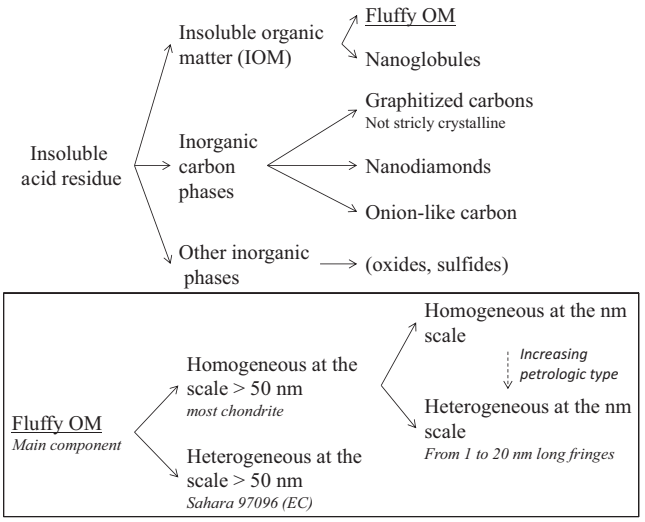

Fig. 1. Terminology and classification of the different materials encountered in the acid residues during this study based on HRTEM imaging. The first level of classification is based on the main elemental composition (organic and inorganic carbon phases, other noncarbonaceous inorganic phases). The second one is based on nanostructural criteria after HRTEM observation (nanoglobules versus fluffy OM, for instance). Finally, the last one (bottom), reveals the different level of structural heterogeneities within the fluffy OMs described in detail in the text. They are highly dependent on the scale of observation and are also based on HRTEM images.

Additional levels of complexity are found within the fluffy disordered OM (Fig. 1, lower part). First, in most chondrites the "fluffy OMs" appear structurally and nanostructurally homogeneous at a scale of approximately 50 nm. However, in Sahara 97096, structural and nanostructural heterogeneity at this scale is much more significant. It precludes the identification of its structure. Second, as petrologic type increases, the structural heterogeneity of the fluffy OM progressively increases at the nanometer scale. The various degrees of multiscale organization observed and the proposed associated terminology are based on the present HRTEM study. We do not claim it to be relevant at all scales or for all analytical techniques, but only for the chondritic IOM studied in the present article.

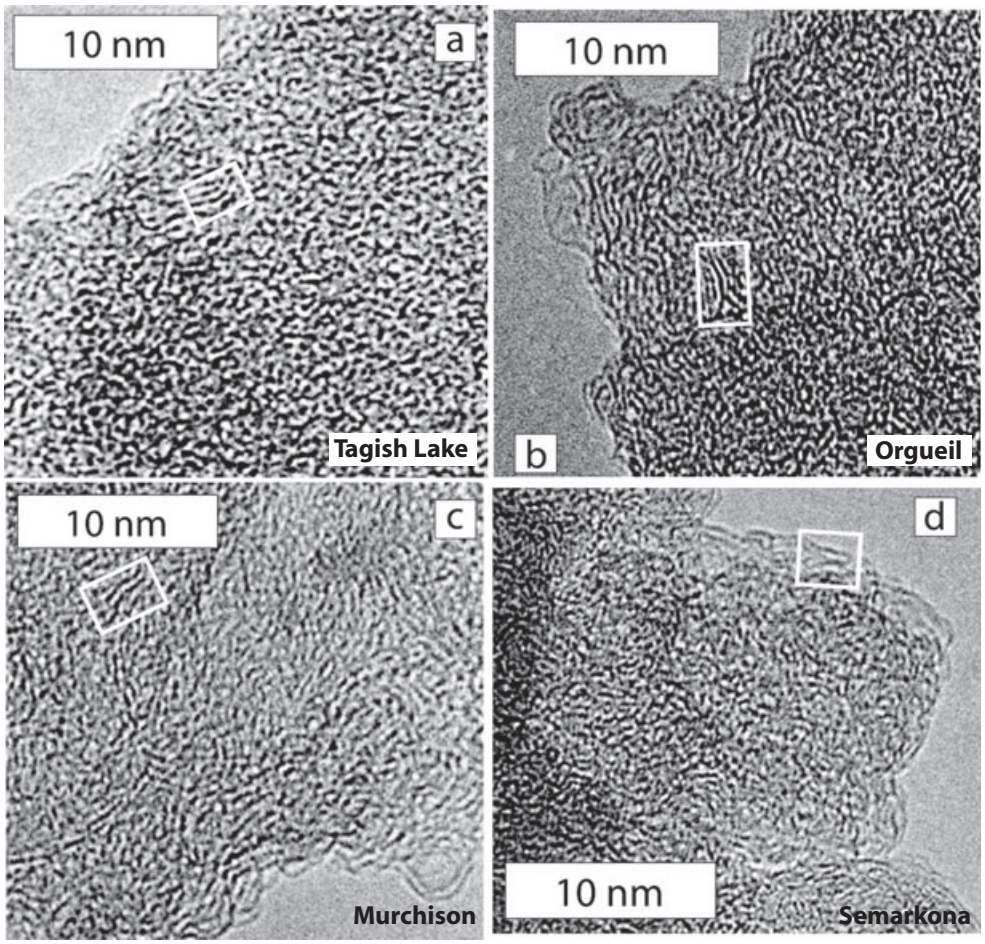

Fig. 2. High resolution transmission electron microscopy images of the "fluffy OM" of the most pristine meteorites: a) Tagish Lake; b) Orgueil; c) Murchison; and d) Semarkona. Most of the fringes are shorter than 1 nm. White rectangular areas correspond to regions where 2 or 3 layers are stacked.

Nature and Evolution of the "Fluffy Organic Matter" along Increasing Petrologic Types

On the basis of their structural and nanostructural similarities, consistent with the absence of significant metamorphism, Tagish Lake (Fig. 2a), Orgueil (Fig. 2b), Murchison (Fig. 2c), and Semarkona (Fig. 2d) are grouped together. They display highly disordered fluffy carbon particles made of polyaromatic layers ≤1 nm in average. Although these layers are mostly randomly oriented, they are sometimes stacked by two or three (see rectangular areas on Fig. 2). These observations are consistent with previous studies of Orgueil (Derenne et al. 2005; Garvie and Buseck 2006), Murchison and Tagish Lake (Derenne et al. 2005, 2006). Structures and nanostructures in Semarkona (LL3.0) are described here for the first time. The structures of these fluffy OM, as seen by HRTEM, appear similar, whereas their elemental composition (Table 1) and Raman spectra (at least for Semarkona) are different (Quirico et al. 2003, 2005a, 2009; Alexander et al. 2007). Indeed, hydrogen and nitrogen abundances in the Semarkona IOM are lower, and its Raman spectrum shows a slightly more evolved material than in Orgueil, Murchison, and Tagish Lake (less fluorescence background and narrower D-band).

The lengths of the fringes (L) in the HRTEM images, the spacing in pairs of parallel fringes, and the height of the coherent domains (d < 0.6 nm, parallelism tolerance +/− 15°) have been previously determined in the fluffy OM from Orgueil, Tagish Lake, and Murchison by using an image analysis software (Rouzaud and Clinard 2002; Derenne et al. 2005; Rouzaud et al. 2005). A mean fringe length (L) smaller than 0.6 nm, coherent domains height (Lc) of about 0.6 nm, and interlayer spacing d_{002} of about 0.48 nm, were reported. We have performed similar image analysis on Semarkona fluffy OM. Figure 3 shows an example

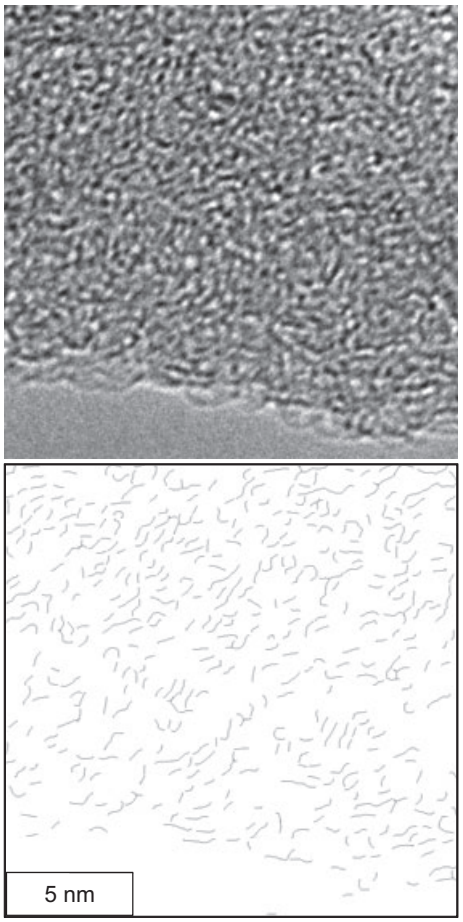

Fig. 3. Example of a HRTEM image from Semarkona typical fluffy OM (top), and associated skeletonized image used for the image analysis (bottom).

of an original HRTEM image and its associated skeletonized image. We obtain a mean fringe length of 0.6 nm and a mean interlayer spacing d_{002} of 0.44 nm. For comparison, crystalline graphite is made of perfectly planar polyaromatic layers spaced by a d_{002} of 0.3354 nm (theoretical value). These values are very similar to previously published values on Orgueil, Murchison, and Tagish Lake (Derenne et al. 2005; Rouzaud et al. 2005). They are significantly different from the values reported by Rietmeijer and MacKinnon (1985), who found much longer fringe length (>6 nm in Orgueil). It is worth noting here that those meteorites are breccia that may include different lithologies and could explain this apparent discrepancy. However, we observed a large number of particles from our samples and they all showed similar nanostructures.

In the fluffy OM of chondrites of petrologic type >3.0, the average degree of organization progressively increases along metamorphism, and is accompanied by the development of a structural and nanostructural heterogeneity, at the scale of a single 100 nm^2 image (Figs. 4 and 5). Whereas in petrologic type <3, fringe length is mostly comprised between 0.246 nm (the lower theoretical limit defined by the size of an aromatic ring) and 1 nm, we observe in Allende a range that goes from 0.246 nm to almost 20 nm. Because of this heterogeneity of the fringe length, we were not able to obtain satisfying averaged data from the software image analysis. This is due in part to the fact that the software developed by Rouzaud and Clinard (2002) was designed to be applied to structurally and nanostructurally homogeneous material, as soot. Moreover, HRTEM images are based on electron diffraction, and the relationship between the size of the structure (layer, domain, and so on) and the tolerance on the Bragg angle adds a strong bias when variable sizes are present in a material, as is the case here. Indeed, the smaller the structure, the higher the tolerance on the Bragg angle. Consequently, small layers will yield fringes (phase contrast) even when they are not well oriented in parallel to the electron beam, and this effect will progressively fade with increasing fringe sizes, for which the Bragg conditions become stricter. Longer individual fringes which are usually wrinkled will produce fringes with a heterogeneous gray level, depending on the interference error, i.e., the deviation of each portion of layer with respect to the exact Bragg angle. Therefore, after the binarization required for the image analysis, the continuous layers unfortunately appear fragmented in the skeletonized images. Altogether, as smaller fringes will be over-represented and longer fringes will be under-represented, significant biases on the average fringe length and coherent domain size are obtained when the analysis procedure is performed on an image with such continuous but wrinkled layers and heterogeneous layer size. It was therefore not possible to compare averaged structural parameters for the low petrologic type IOM with the higher ones. Instead, we chose to use a more qualitative approach to describe the fluffy OM in petrologic types >3 by reporting visual estimations and ranges of structure sizes or fringe lengths.

In chondrites of intermediate petrologic types (approximately 3.1–3.4), the structural order of the fluffy OM increases along metamorphism. Figures 4a and 4b show typical examples of the structure observed in Leoville (CVRed) and Kaba (CVOx) chondrites. They both display the same features (1) mean fringe length between 1 and 3 nm, i.e., slightly longer than the fringe length in the type 1 and 2 chondrites; and (2) a stacking increase, with a number of parallel fringes up to 5 on.

Acid residues from all ≥3.6 petrologic type chondrites (Fig. 5) display a similar fluffy OM. The organization degree is higher than in IOMs of petrologic type 3.1 chondrites and the fringe length also increases

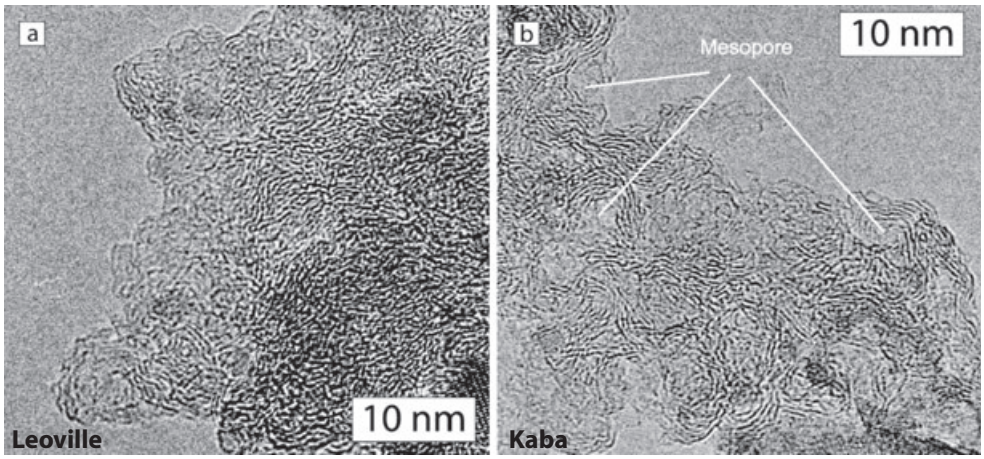

Fig. 4. High resolution transmission electron microscopy images of the fluffy component of IOMs from 3.1 chondrites: a) Leoville (CV_{Red}); b) Kaba (CV_{Ox}). The fringes are longer than in lower petrologic types and sometimes stacked by up to five layers.

with petrologic type. Whereas the fringe length is almost homogeneous in types 1 and 2, it covers a wide range in type ≥3.6 IOMs, from less than 1 nm to more than 10 nm. Most fringes have a size ranging from 5 to 10 nm. The proportion of nonstacked layers decreases, and the number of stacked fringes is higher (up to 10). Two subgroups, also characterized by distinct Raman spectral parameters (Figs. 5 and 6), can be distinguished among the type ≥3.6 chondrites we studied. The IOMs of Tieschitz (H), Kainsaz (CO), and Mokoia (CV_{Ox}) (approximately 3.6) seem to exhibit a lower number of parallel fringes than the IOMs of Ornans and Allende (≥3.6). To summarize these evolutions, we plotted the fringe length estimation together with the full width at half maximum of the D-band (FWHM-D) of the Raman spectra reported by Bonal et al. (2006, 2007). Raman data are lacking for CIs and CMs. With increasing petrologic types, the increase of the fringe length is correlated with the decrease of the FWHM-D.

In addition to the abundant fluffy OM, nanoglobules have been found in chondrites from the whole range of petrologic types (Table 1), i.e., in Orgueil, Murchison, Tagish Lake, Semarkona, Kainsaz, and Sahara 97096. They are probably also present in other IOMs, but may just not have been seen in the course of this work. Interestingly, they often occur aggregated together, which has also been observed in situ in matrices of CR chondrites for instance (Le Guillou and Brearley 2010).

Heterogeneities within a Given Chondrite

In the acid residues of type ≥3.6 chondrites and of the enstatite chondrite Sahara 97096, the degree of multiscale (structural and nanostructural) organization, from particle to particle is more heterogeneous than in residues of lower petrologic type chondrites. Indeed, various additional nanostructures can be found in addition to the main fluffy OM. Tieschitz and Allende are described as examples of this heterogeneity (Figs. 7 and 8). In Sahara 97096, the heterogeneity is even stronger and it was impossible to identify representative images of the fluffy OM (Fig. 9). Each specific case is developed in the next paragraphs.

In Tieschitz, a nanostructure clearly different from the main fluffy OM (Fig. 5a), was observed (Fig. 7). In the area imaged on Fig. 7, the fringes can be as long as 20 nm, whereas the main fluffy OM usually has fringes shorter than 10 nm on average (Fig. 5a). In addition, they form a mesoporous nanostructure, with more or less straight angles between the pore walls (made of layer stacks), depending on particles.

Nanostructural heterogeneity is also frequently observed in the acid residue of Allende (Fig. 8). Lamellar nanostructure tends to develop allowing the occurrence of partially graphitized particles, showing continuous and planar polyaromatic layers as long as 100 nm, stacked by up to 20. Such nanostructure is present in the acid residue next to the main fluffy OM, characterized by fringes shorter than 10 nm. Furthermore, the curved particle present in the lower part of Fig. 8a is itself structurally heterogeneous. Indeed, a higher degree of organization is found in the outer part of the convexity of the object, as shown by the close-up in Fig. 8b.

The enstatite chondrite Sahara 97096 is classified as a 3.1–3.4 petrologic type on the basis of Raman spectra measured in the matrix (Quirico et al. 2011). However, Sahara 97096 is different from other chondrites as it is characterized by a range of degrees of organization, from amorphous-like to graphitized particles. This prevented

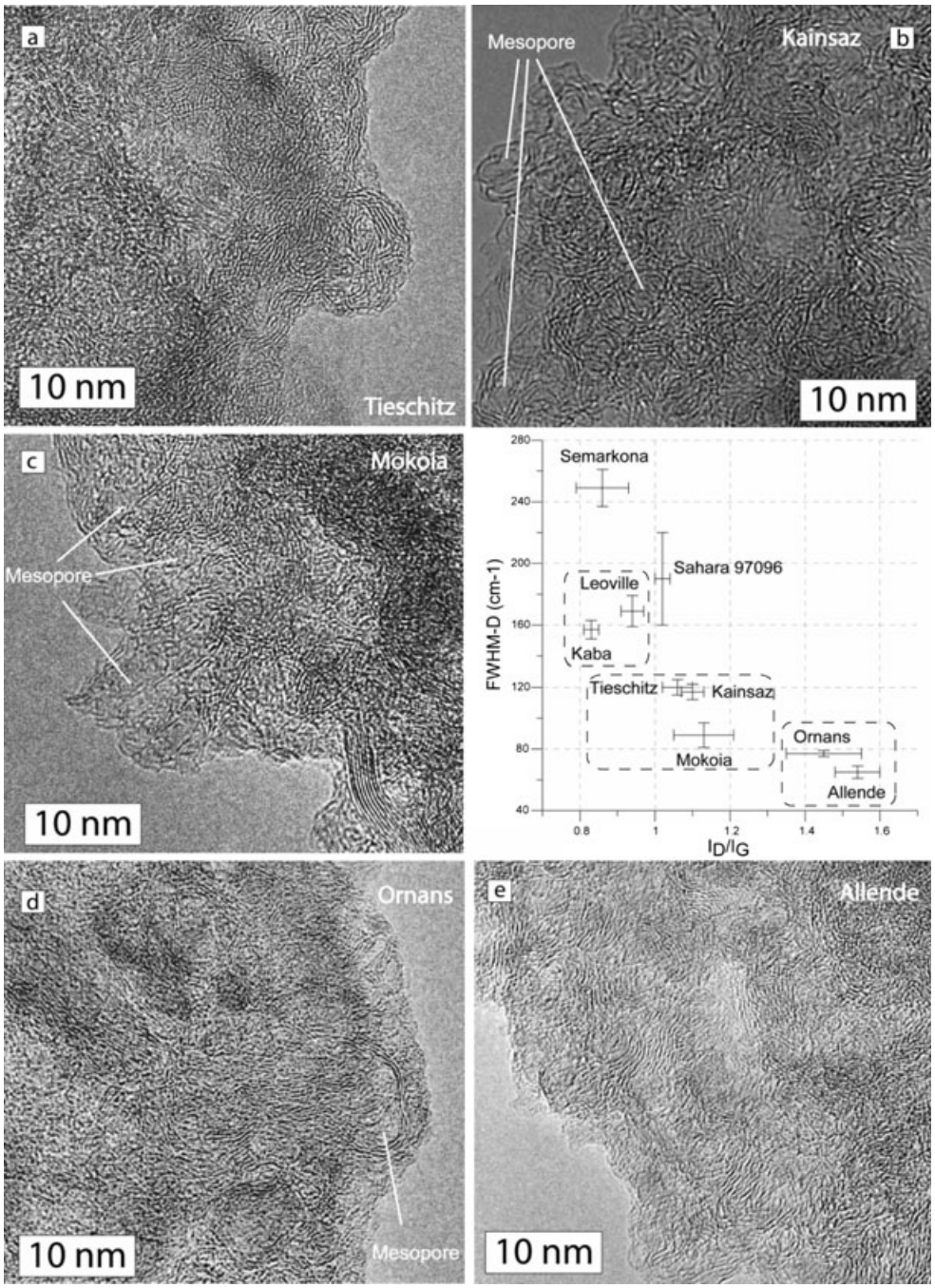

Fig. 5. High resolution transmission electron microscopy images of the fluffy OM in chondrites from petrologic type ≥3.6: a) Tieschitz; b) Kainsaz; c) Mokoia; d) Ornans; e) Allende; and a plot of the Raman spectra parameters (full width at half maximum of the so-called D-band [FWHM-D] versus I_D/I_G, intensity ratio of the D and G bands) for all the studied chondrites. Raman data are taken from Quirico et al. (2003) and Bonal et al. (2006, 2007). Ornans and Allende present particularly long and stacked fringes, consistent with their higher degree of structural organization inferred from Raman analysis.

us from identifying representative illustration of fluffy OM as we did for the other chondrites. Figure 9a displays a 100 nm large graphitized carbon particle with a high degree of structural organization, as reflected by the presence of about 100 continuous stacked layers. However, this nanostructure appears to be only a minor component of the residue. Intermediate structures, classified by decreasing organization degrees, are shown on Figs. 9b–d. Although polyaromatic layers on Fig. 9b are clearly shorter than the ones in Fig. 9a, a preferential

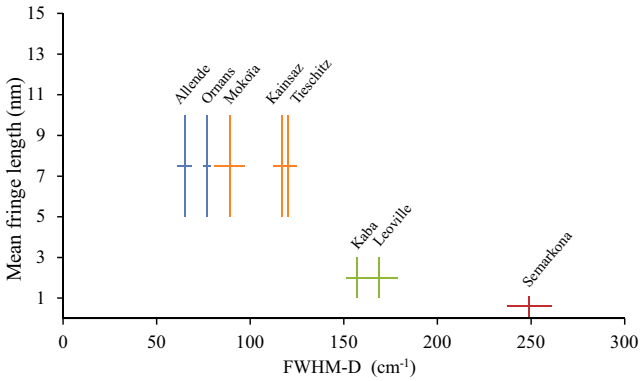

Fig. 6. Mean size range of the fringe length plotted versus the FWHM-D extracted from Raman spectra of the corresponding meteorites (from Bonal et al. 2006, 2007). A variation of the FWHM-D by a factor of 3 corresponds to an increase of the fringe length by about an order of magnitude.

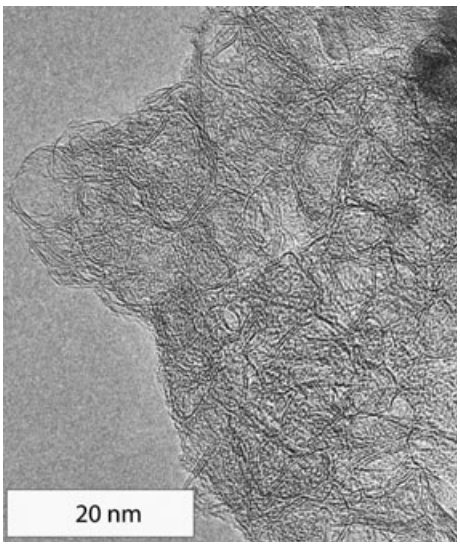

Fig. 7. High resolution transmission electron microscopy image from Tieschitz IOM. This carbon material, made of stacked, curved and long polyaromatic layers, is clearly structurally different from the main population of fluffy OM. This illustrates the structural heterogeneity of the carbon material within a given meteorite.

planar orientation of the BSUs is visible. Figures 9c and 9d show smaller, nanometer-sized BSUs than Figs. 9a and 9b. The BSUs are randomly oriented on Fig. 9d. This very disordered material is structurally similar to the fluffy OM from type 3.1 carbonaceous chondrites (Fig. 4).

Onion-Like Carbons

In addition, rare onion-like carbons have been detected in three acid residues (Fig. 10), all from petrologic type ≥3.1 chondrites. These onion-like carbons are smaller than 10 nm, made of two to five closed and concentric polyaromatic layers, and show internal voids. Their presence was previously reported in Allende (CV_{Ox}) by Harris et al. (2000) and in Kainsaz by Remusat et al. (2008). In the present work, we describe them in one additional chondrite from a different chemical group, Sahara 97096 (EH). We also confirm their presence in Allende and Kainsaz (CO). These observations, taken together reinforce the previous conclusions that they are not anthropogenic pollution on the TEM grids.

DISCUSSION

The HRTEM observations of a large set of chondritic acid residues lead us to define four main carbonaceous components. They are present in most of the studied chondrites. These components are (1) a highly disordered carbonaceous material called "fluffy OM"; (2) more or less graphitized particles; (3) onion-like carbons; and (4) structurally highly disordered nanoglobules. In the following, we discuss the respective possible origins and parent body evolutions of three of these components. We do not include the nanoglobules in the discussion as they have been the subject of previous works (Garvie and Buseck 2004, 2006). The main observations and interpretations are that (1) the observed structural development are correlated with previous Raman spectroscopy analysis (Quirico et al. 2003; Bonal et al. 2006, 2007; Busemann et al. 2007); (2) for a given petrologic type, the structure and nanostructure of the "fluffy OM" are similar (with the exception of the enstatite chondrite Sahara 97096). It suggests that OM precursors were structurally similar and that comparable subsequent parent body thermal evolution (pressure, grain size, heating duration and so on) occurred among the different chemical chondritic groups; (3) the acid residue of the enstatite chondrite Sahara 97096 appears to be different from other chondrites, which implies a specific history for this sample; (4) onion-like carbons are scarce, but systematically present. We discuss their possible origin.

Similarity of the IOM among Chondrite Groups and Evolution along Metamorphism

Fluffy OM From Petrologic Type ≤3 Chondrites

The structure and nanostructure of the fluffy OM from the most primitive objects (Orgueil, Tagish Lake, Murchison, and Semarkona) are similar at the TEM scale. This observation indicates that their respective precursors were probably structurally similar and that their different aqueous and thermal histories did not

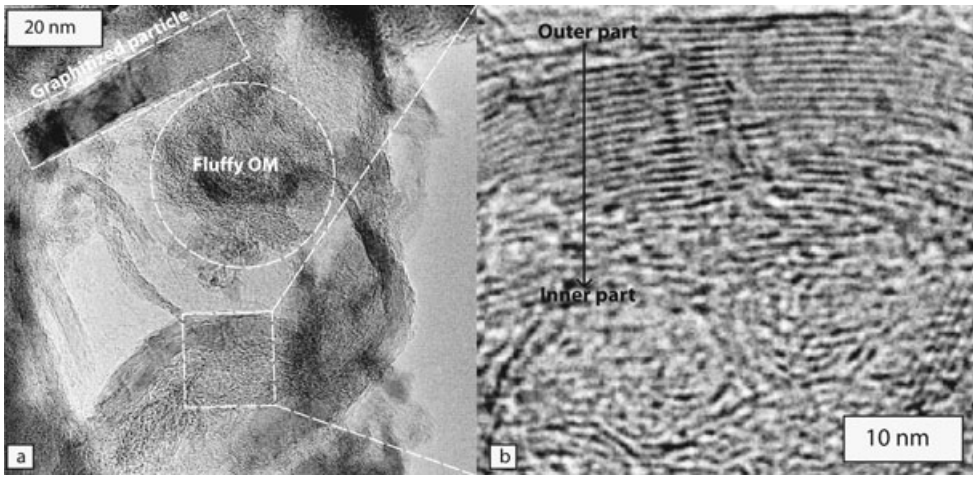

Fig. 8. a) High resolution transmission electron microscopy images of submicrometer sized particles with very different degrees of organization in the IOM of Allende. The fluffy OM is similar to the material imaged in Fig. 5e. Better organized ("graphitized") nanoparticles are also present). b) Close-up image of the white rectangular area shown on Fig. 8a. This curved particle is better organized in its outer part than in its inner part.

significantly influence their structural evolution. Their polyaromatic layers are small (< 1 nm), randomly oriented and mainly unstacked (Figs. 2 and 3) (Derenne et al. 2005; Garvie and Buseck 2006). The structure of the organic matter from the three aqueously altered meteorites (Orgueil, Murchison, Tagish Lake) are expected to be similar as they all escaped significant heating. Interestingly, Semarkona, less altered and probably more heated, also exhibits similar structure and nanostructure for its fluffy OM at the scale of HRTEM imaging. However, the Raman spectra of these chondrites are different (smaller full width at half maximum for its defect band; FWHM-D = 228 ± 20 cm^{-1} for Semarkona compared to FWHM-D > 300 ± 30 cm^{-1} in Orgueil and Murchison; Quirico et al. 2003, 2005a). As the bulk composition of the acid residue from Semarkona shows lower H/C and N/C ratios than in Orgueil and Murchison (Alexander et al. 2007), the discrepancy between Raman and TEM results may suggest that the spectral differences mainly originate from the chemistry and the nature of the functional groups. Indeed, the polyaromatic structures, as seen by HRTEM, are similar. This implies that the maximum temperature possibly encountered by Semarkona (260 °C; after Alexander et al. 1989) does not permit the growth of the aromatic layers above the resolution threshold attainable by high resolution TEM. This is usually also the case for terrestrial coals, which evolve chemically, but are almost not structurally modified (i.e., without noticeable layer length change) below 200 °C, as imaged by HRTEM. Furthermore, Murchison and Orgueil may have been subjected to different alteration temperatures, respectively, up to 80 °C (Baker et al. 2002) and up to 150 °C or more (Zolensky et al. 1989). However, their fluffy OMs do not record detectable structural differences. Conclusively, the similar structures and nanostructures of the fluffy OM thus strengthen the assumption that these meteorites accreted precursors similar from the structural point of view (even if their isotopic and molecular compositions may have been different), which were not significantly modified by aqueous or thermal processes in the temperature range 80–260 °C.

Increasing Organization Degree along Metamorphism

From chondrites of petrologic types 3.1 to 3.6, the fluffy OM becomes progressively more organized (Figs. 2–6), probably under the influence of the parent body thermal metamorphism. HRTEM provides an estimation of the evolution of the polyaromatic layer sizes. They grow from less than 1 nm in chondrites of petrologic type ≤3.0 to less than 3 nm in type 3.1 chondrites and are finally in the range 5–10 nm in type 3.6 chondrites, the longest fringes reaching 20 nm. This growth is accompanied by a higher number of stacked layers.

These fluffy OM are characterized by a turbostratic biperiodic order that is clearly different from the triperiodic order of perfect graphite. Hence, this structural evolution should not be called "graphitization" as it mainly involves carbonization. This process, in terrestrial coals for instance, consists of the progressive loss of H, N, and O atoms (Rouzaud and Oberlin 1990). In chondrites, however, only H and N are lost in the course of metamorphism (H/C ratio decrease from 0.8 to 0.1 between type 1 and type 3.6

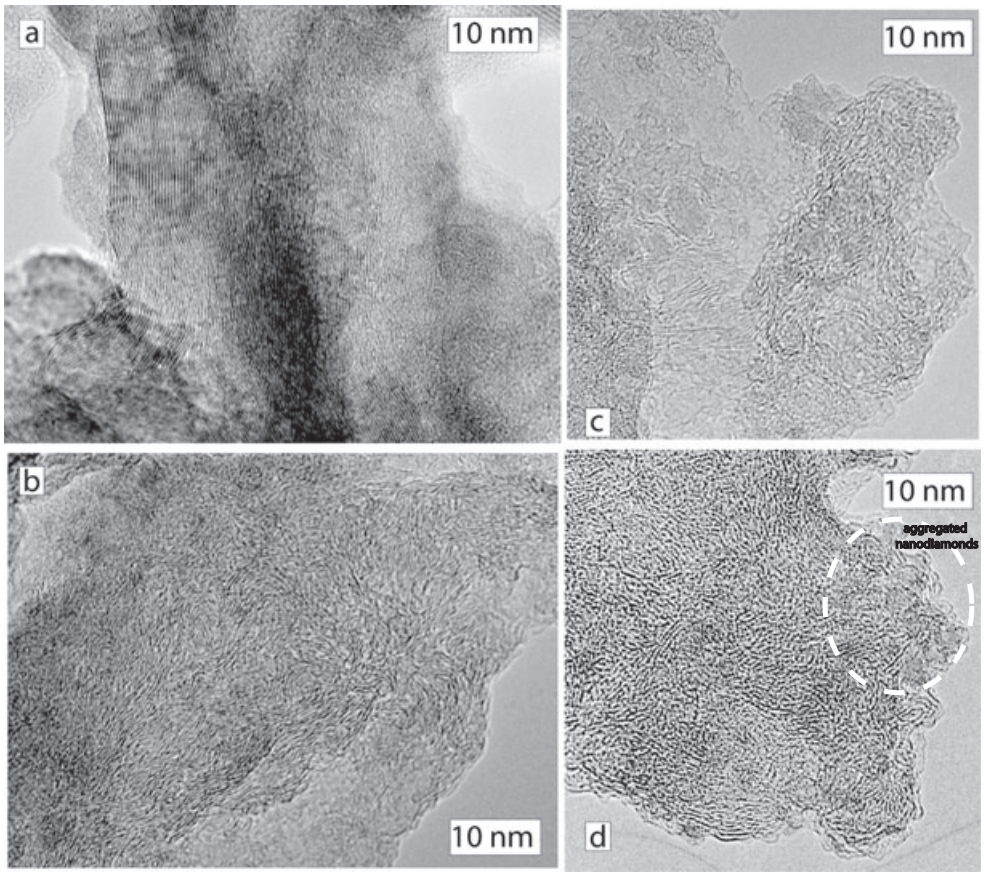

Fig. 9. Transmission electron microscopy images of Sahara 97096 IOM illustrating its nanostructural diversity. a) A well-organized carbon particle with long (about 100 nm in size) and well-stacked polyaromatic layers. Such a particle is structurally far from the crystalline order of graphite, as the fringes are frequently disrupted and undulated; b) a region where the organization degree is lower than in (a), but with fringes nevertheless roughly oriented along the same direction; c) a portion of the IOM where stacking degree of the polyaromatic units is lower than in previous images (shorter fringes, stronger disorientation, and larger distribution of the interlayer spacing); d) an area with shorter and randomly oriented fringes (nanometer-sized). It represents a lower end-member in terms of degree of structural organization. Note, however, that such a phase is not amorphous as polyaromatic layers are present. In addition, nanodiamonds, identified through their d_{111} interlayer spacing (0.206 nm) are observed (circled).

chondrites), whereas O seems to be retained (Alexander et al. 2007).

This is in contrast with terrestrial systems where O is usually among the first hetero-atom to be lost. Two possible reasons may account for this discrepancy (1) the different nature of the precursors (more frequent stable oxygen bridges in chondritic IOM) as well as (2) the absence of confinement pressure on the parent body (Quirico et al. 2009).

Both Raman spectroscopy and TEM are sensitive to the degree of structural organization of the chondritic carbonaceous matter, but at a different scale. Indeed, the improvement of the degree of organization along increasing petrologic type seen by HRTEM is consistent with previous conclusions obtained by Raman spectroscopy (Bonal et al. 2006, 2007; Busemann et al. 2007). We show here that the whole evolution range described by Raman parameters between petrologic type 1 and type 3.6 corresponds to a noticeable, but limited development of the size of the polyaromatic layers, not exceeding a few nanometers. The increased size of polyaromatic domains in the petrologic type >3 are consistent with the previous observation in the same meteorites of increased intensity of the 1s-σ* exciton (Cody et al. 2008) that is shown to correlate with an increase in the number of delocalized electrons. The "1s-σ* exciton" absorption band was attributed in graphite to the presence of planar domains of highly conjugated graphene sheets (Batson 1993).

In agreement with previous works (Bonal et al. 2006, 2007; Alexander et al. 2007; Cody et al. 2008; Remusat et al. 2008; Quirico et al. 2009), we suggest that this evolution, correlated with petrologic type, is controlled by the extent of parent body thermal metamorphism. In this

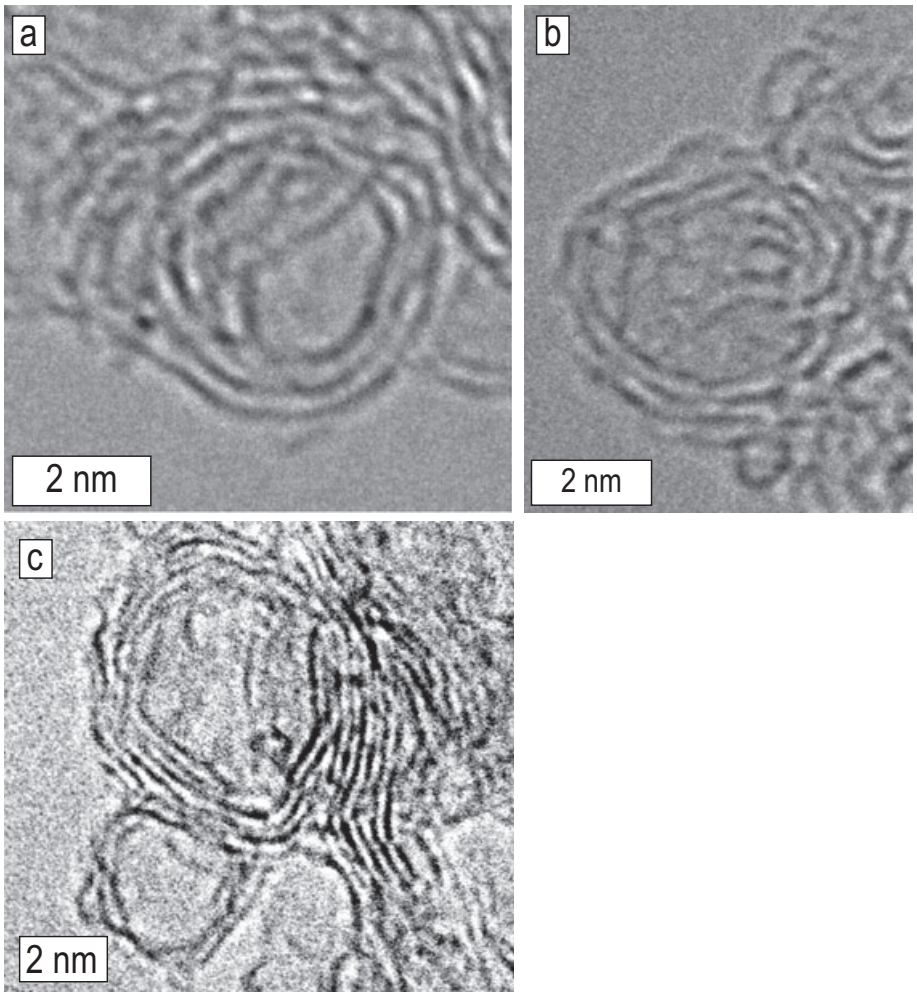

Fig. 10. Onion-like carbon observed in a) Kainsaz, b) Sahara 97096, and c) Allende.

study, HRTEM data, when compared with terrestrial IOMs and laboratory heating experiments, add a line of evidence to the previous conclusions based on chemistry and spectroscopy data. The observed nanostructures, which are similar in all chondrite groups (with the exception of the enstatite chondrite Sahara 97096, discussed below), can only be produced by heating over long time scales.

The parameters controlling carbonization, subsequent structure improvement, and finally graphitization are the chemical and structural nature of the precursor, the pressure, the heating duration, and the temperature (Deurbergue et al. 1987; Oberlin 1989; Beyssac et al. 2002, 2003; Bonal et al. 2006). In chondritic IOMs, the high reticulation degree of the polyaromatic moieties, maintained by cross-linkers, such as oxygen, is responsible for their random orientation and gives a nongraphitizing character to the precursor. This implies that graphite cannot be obtained without applying confinement pressure (Oberlin 1989; Beyssac et al. 2003). The latter is generally considered negligible within asteroidal parent-bodies, due to their small size and low gravity (Bennett and McSween 1996). Temperature and heating duration are therefore the main parameters controlling the evolution of the IOMs in chondrites, and we discuss below their relative influences.

If it is clear that temperature mainly controls carbonization and graphitization processes, an important kinetic barrier is associated with the sluggish graphitization mechanism, and heating duration should also be considered (Beyssac et al. 2003). Geological time scales may be necessary to overcome some of the reaction steps (loss of heteroatoms, polyaromatic layer growth, defect resorption, stacking development, and, finally, establishment of a three dimensional organization). Indeed, at atmospheric pressure, high temperature laboratory pyrolysis ($T > 2600$ °C) of nongraphitizing material, such as saccharose-based chars, yield highly disordered carbon

if confinement pressure is not applied (Rouzaud and Oberlin 1989; Beyssac et al. 2003; Bernard et al. 2010). Even if these synthetic carbons are not produced by the same processes as chondritic IOM, they are structurally similar enough to be used for comparison of their graphitization behavior.

For instance, the pyrolysis of Orgueil IOM at 1000 °C yields a degree of structural organization much lower than what is observed in Allende, whereas Allende parent body has not been heated to such a temperature on its asteroidal parent body. Therefore, if one assumes that chondrites have structurally similar precursors, long heating duration is probably necessary, in the absence of pressure, to reach the organization degree of the fluffy OM observed in the higher petrologic types. We conclude that the nanostructure observed in petrologic type >3.1 chondrites are not likely to be produced by short-time scale heating events (shock metamorphism, Le Guillou et al. 2010; or nebular transient heating for instance), and that the most plausible thermal event is a long-term heating, compatible with the ^{26}Al decay on the parent body over millions of years (Bennett and McSween 1996).

A given structural organization degree, as quantified by Raman spectroscopy, could potentially be obtained by different combinations of duration/temperature conditions of thermal treatments. However, the direct observation of the carbon nanostructures by HRTEM shows that chondritic IOMs from all chemical groups display similar structures and nanostructures for a given petrologic type, which is a strong indication that chondrites (1) accreted precursors relatively similar in terms of structures, (2) recorded comparable temperature-duration pathways (with the exception of Sahara 97096, see below).

Origins of Heterogeneities within Fluffy OM of Petrologic Types >3.0

Along petrologic types, the fluffy OM evolves from relatively homogeneous compact residues to assemblages of more structurally and nanostructurally heterogeneous particles. We can divide this heterogeneity into two groups. The first one corresponds to the development of a structural heterogeneity within the fluffy OM itself. It is illustrated by images of fluffy OM from petrologic types >3.6, which show a wider distribution of fringe length, as well as a more variable number of stacked fringes from one particle to the other (Fig. 5). The second type of heterogeneity occurs at a larger scale (greater than approximately 50 nm) and relates to the presence of particles with a clearly higher structural organization degree and showing different nanostructures (mesoporous and lamellar) as described in Allende (Fig. 8).

Laboratory experiments, such as pyrolysis under pressure (Beyssac et al. 2003) or iron-catalyzed graphitization at temperature above 1150 °C have shown that structural and nanostructural heterogeneities are systematically produced. Heterogeneities are also observed in terrestrial metamorphism (Deurbergue et al. 1987). This inherent nature of the carbonaceous material behavior along metamorphism could explain some of the final heterogeneity of the fluffy OM. However, we propose here two additional processes, specific to chondrite metamorphism, which could also contribute to this heterogeneity.

First of all, carbon grains in chondritic matrices are characterized by variable sizes from the submicron scale to below the nanometer scale (Brearley 1999; Floss and Stadermann 2009; Le Guillou et al. 2011). We suggest that the initial size distribution, for a given time-temperature metamorphic pathway, influences the final size distribution and structural parameters of the polyaromatic layers. Very small particles scattered through the inorganic materials of the matrix cannot grow as much as the larger one, thus producing layers of heterogeneous sizes. This mechanism would also imply that the initial particle size distribution, at the onset of metamorphism, could be an important parameter influencing the structural evolution of the IOMs: the larger the initial particles, the higher the final averaged graphitized domains potentially attainable. Furthermore, we suggest that the mineral environment may also play a role, by orienting the growth of the aromatic layers along its surfaces (template effect). This surface-controlled growth mechanism is observed experimentally during the carbonization of silicates-associated organic matter (Beguin et al. 1996; Zhai et al. 2008). The long and continuous fringes observed in Tieschitz (Fig. 7) show angles and appear like they grew around a faceted mineral, supporting this hypothesis. We may consequently infer that the mineral environment plays a role, as IOM scattered through chemically and morphologically heterogeneous phases could produce heterogeneous nanostructures.

The second category of heterogeneities (e.g., the presence of graphitized particles), which had already been described in previous work (Smith and Buseck 1981; Brearley 1990; Vis et al. 2002; Remusat et al. 2008) is difficult to reconcile with low temperature parent body metamorphism, and may rather relate to high temperature processes. It is indeed unlikely that metamorphism would have produced such a high graphitization degree on a limited number of particles, especially because we have not observed intermediate graphitization degree between the fluffy OM and those particles. In contrast, graphitized particles have previously been reported in ordinary and carbonaceous chondrites by Raman and

TEM, and are associated with metal (Brearley 1990; Mostefaoui et al. 2000, 2005). Some of these metal/graphitized particle associations were sometimes even found in close contact with chondrules, for instance in Bishunpur (Mostefaoui et al. 2000). At this point, even if it is not possible to completely exclude metal-related parent body metamorphism, it is more probable that the particles observed in our residues have been formed by metal-catalyzed reactions at high temperature prior to parent body accretion, a mechanism which is experimentally supported (Audier et al. 1981; Audier and Coulon 1985; Charon et al. 2011). Xenoliths with different thermal history, included within the host meteorite, and carrying graphitized particles could account for the heterogeneity. However, the chondrule forming event would better fit those observations, and especially the carbon metal association found by previous authors.

A Different History for Carbons in Sahara 97096 (EH3)?

From the HRTEM point of view, the acid residues of Sahara 97096 appear more complex than the other ones described in this work. Indeed, the degree of observed structural heterogeneity in the carbonaceous matter from Sahara 97096 is higher and occurs at a different scale than in other chondrites (Figs. 1 and 9). Nearly amorphous materials coexist with more developed BSUs and graphitized lamellar nanostructures. It consequently appeared impossible to identify a representative illustration of the fluffy OM with HRTEM images covering only 50×50 nm areas. Raman spectroscopy, on the other hand, does not reveal the structural heterogeneity observed at the nanometer scale by TEM. Raman spectra, as measured in several matrix areas, are reproducible and comparable in average to spectra from type 3.1–3.4 chondrites (Robin et al. 2008; Quirico et al. 2011). This apparent homogeneity is probably due to the fact that Raman spectra reflect the average organization degree at the micrometer scale, thus including several different particles.

In addition, although graphitized particles (Fig. 9a) are more commonly found in the acid residue of Sahara 97096 than in other chondrites, Raman spectra measured in the matrix only revealed the presence of disordered carbonaceous material. No spectra of graphitized particles were observed by Quirico et al. (2011). Thus, the graphitized particles may not be located in the fine-grained matrix, but possibly associated with large metal grains (or xenoliths, less likely). The chemical treatment used to isolate the carbon phases would then result in a mixing of these diverse carbon occurrences. Associations of large metal grains and graphitized particles have been described by Rubin and Scott (1997) in several enstatite chondrites and attributed to localized, shock-induced, partial melting events. Piani et al. (2010, 2012) described these associations in Sahara 97096. In the case of partial melting, metal will play a catalytic role (Oberlin and Rouchy 1971; Charon et al. 2011). Dissolution of disordered carbon in liquid metal (carbon-metal eutectic at approximately 1150 °C) followed by exsolution of graphite upon cooling is a way of producing graphite (Austermann 1968). This graphitized component may have a significant contribution on the bulk elemental composition of the acid residue of enstatite chondrites. As it must be mostly hydrogen, oxygen, and nitrogen free, we infer that it would consequently reduce the bulk H/C, N/C, and O/C ratios. The H/C composition of Sahara 97096 is 0.31 (Piani et al. 2012). It is just slightly higher, but consistent with IOM of other enstatite chondrites which have low H/C, N/C, and O/C compared with carbonaceous and ordinary chondrites (Alexander et al. 2007). Thus, organized carbons associated to metal might represent a nonnegligible fraction of the final carbon particles of enstatite chondrites. The catalytic behavior of metal, abundant but heterogeneously distributed in enstatite chondrites, would lead to carbon grains with a much higher structural degree than the most abundant IOM. This would explain (1) the high degree of organization of some carbon particles, and (2) the high level of heterogeneity observed within the acid residue of Sahara 97096. This could likely be a common characteristic of enstatite chondrites.

Origins of the Onion-Like Spherules

The onion-like spherules observed in diverse chondrites are characterized by a similar size, between 5 and 10 nm and are made of less than five concentric and continuous graphene layers with internal voids (Fig. 10). They could be the product of nanodiamond graphitization during thermal events, either in the nebula or in the parent body. Huss and Lewis (1995) and Huss et al. (2003) showed that the abundance of nanodiamonds decreases during both nebular thermal events and gradual parent body metamorphism. Experimental nanodiamond pyrolysis is known to produce onion-like carbons above 1000 °C (Butenko et al. 2000; Tomita et al. 2002; Kuznetsov and Butenko 2006; Le Guillou et al. 2009), and their typical sizes and morphologies resemble the particles observed in the present study. Furthermore, Le Guillou et al. (2009) have shown, on the basis of an experimental kinetic study of synthetic nanodiamond pyrolysis, that onion-like structures can be formed either during high temperature–short duration events (1300–1500 °C, minutes to hours) or possibly during low temperature–long

duration events (< 300 °C, millions of years). These two sets of temperature–duration conditions are relevant for both nebular and parent body thermal events, and consistent with Huss et al.'s (2003) scenarios. The nanodiamonds could thus be transformed into onion-like carbons through thermal events.

CONCLUSION

The dominant "fluffy OM," nanoglobules, graphitized particles, nanodiamonds, and the onion-like structures are observed in most of the chondritic acid residues. The only exception is the enstatite chondrite Sahara 97096 where the structural and nanostructural heterogeneities are much higher. This work extends the number of meteorites where such a range of different carbon phases is observed.

The disordered fluffy OM shows a structural organization improvement along a series of chondrites with increasing petrologic types, which correlates with Raman spectroscopy analysis. This structural evolution probably results from parent body thermal metamorphism. For a given petrologic type, but independently of the chondrite group, the structure and microporous nanostructure of the carbonaceous material are similar. This reinforces the idea that they accreted structurally and nanostructurally similar precursors and then were submitted to similar conditions of metamorphism (temperature–duration–pressure). We suggest that the initial size of the organic particles, as well as their distribution and relation with the inorganic environment in the matrix, could be the additional parameters controlling and limiting the structural organization degree of the IOMs.

In enstatite chondrites, we have shown that the carbonaceous particles are highly heterogeneous and that the frequent occurrence of graphitized particles could be the result of interactions with molten iron possibly due to localized shock-melting events.

Our HRTEM study illustrates a common feature across all samples: the acid residues are highly heterogeneous and contain carbon phases probably formed at different periods and in different conditions. Their respective history can be in part unraveled by their structural characterization.

Acknowledgments—We are thankful to Sandra Pizzarello, who provided the acid residue of Tagish Lake. Mark Garcia and John Eiler are thanked for providing the acid residue of Semarkona coming from the S. Epstein sample collection at Caltech. Adrian Brearley is also warmly acknowledged for reading through the manuscript and improving the quality of the English.

Editorial Handling—Dr. A. J. Timothy Jull

REFERENCES

Abreu N. M. and Brearley A. J. 2010. Early solar system processes recorded in the matrices of two highly pristine CR3 carbonaceous chondrites, MET 00426 and QUE 99177. *Geochimica et Cosmochimica Acta* 74:1146–1171.

Alexander C. M. O'D., Hutchison R., and Barber D. J. 1989. Origin of chondrule rims and interchondrule matrices in unequilibrated ordinary chondrites. *Earth and Planetary Science Letters* 95:187–207.

Alexander C. M. O'D., Russell S. S., Arden J. W., Ash R. D., Grady M. M., and Pillinger C. T. 1998. The origin of chondritic macromolecular organic matter: A carbon and nitrogen isotope study. *Meteoritics & Planetary Science* 33:603–622.

Alexander C. M. O'D., Fogel M., Yabuta H., and Cody G. D. 2007. The origin and evolution of chondrites recorded in the elemental and isotopic compositions of their macromolecular organic matter. *Geochimica et Cosmochimica Acta* 71:4380–4403.

Amari S., Anders E., Virag A., and Zinner E. 1990. Interstellar graphite in meteorites. *Nature* 345:238–240.

Audier M. and Coulon M. 1985. Kinetic and microscopic aspects of catalytic carbon growth. *Carbon* 23: 317–323.

Audier M., Oberlin A., Oberlin M., Coulon M., and Bonnetain L. 1981. Morphology and crystalline order in catalytic carbons. *Carbon* 19:217–224.

Austermann S. B. 1968. *Chemistry and physics of carbon*, vol. 7, edited by Walker P. L. New York: Marcel Dekker. p. 137.

Baker L., Franchi I. A., Wright I. P., and Pillinger C. T. 2002. The oxygen isotopic composition of water from Tagish Lake: Its relationship to low-temperature phases and to other carbonaceous chondrites. *Meteoritics & Planetary Science* 37:977–985.

Batson P. E. 1993. Carbon 1s near-edge-absorption fine structure in graphite. *Physical Review B* 48:2608–2610.

Beguin F., Rouzaud J. N., Maimoun I. B., and Seron A. 1996. Elaboration and structure of silicate/carbon lamellar nanocomposites. *Journal of Physics and Chemistry of Solids* 57:1019–1029.

Bennett M. E. and McSween Jr. H. Y. 1996. Revised model calculations for the thermal histories of ordinary chondrite parent bodies. *Meteoritics & Planetary Science* 31:783–792.

Bény-Bassez C. and Rouzaud J. N. 1985. Characterization of carbonaceous materials by correlated electron and optical microscopy and Raman microspectroscopy. *Scanning Electron Microscopy* 1:119–132.

Bernard S., Beyssac O., Benzerara K., Findling N., Tzvetkov G., and Brown Jr. G. E. 2010. XANES, Raman, and XRD study of anthracene-based cokes and saccharose-based chars submitted to high-temperature pyrolysis. *Carbon* 48:2506–2516.

Beyssac O., Goffé B., Chopin C., and Rouzaud J .N. 2002a. Raman spectra of carbonaceous material in metasediments: A new geothermometer. *Journal of Metamorphic Geology* 20:859–871.

Beyssac O., Rouzaud J. N., Goffé B., Brunet F., and Chopin C. 2002b. Graphitization in a high-pressure, low-temperature metamorphic gradient: A Raman microspectroscopy and

HRTEM study. *Contributions to Mineralogy and Petrology* 143:19–31.

Beyssac O., Brunet F., Petitet J. P., Goffé B., and Rouzaud J. N. 2003. Experimental study of the microtextural and structural transformations of carbonaceous materials under pressure and temperature. *European Journal of Mineralogy* 15:937–951.

Bonal L., Quirico E., Bourot-Denise M., and Montagnac G. 2006. Determination of the petrologic type of CV3 chondrites by Raman spectroscopy of included organic matter. *Geochimica et Cosmochimica Acta* 70:1849–1863.

Bonal L., Bourot-Denise M., Quirico E., Montagnac G., and Lewin E. 2007. Organic matter and metamorphic history of CO chondrites. *Geochimica et Cosmochimica Acta* 71:1605–1623.

Brearley A. J. 1990. Carbon-rich aggregates in type 3 ordinary chondrites: Characterization, origins, and thermal history. *Geochimica et Cosmochimica Acta* 54:831–850.

Brearley A. J. 1999. Origin of graphitic carbon and pentlandite in matrix olivines in the Allende meteorite. *Science* 285:1380.

Brearley A. J. 2002. Heterogeneous distribution of carbonaceous material in Murchison matrix: In situ observations using energy filtered transmission electron microscopy (abstract #1388). 33rd Lunar and Planetary Science Conference. CD-ROM.

Brearley A. J. 2008. Amorphous carbon-rich grains in the matrices of the primitive carbonaceous chondrites, ALH 77307 and ACFER 094 (abstract #1387). 39th Lunar and Planetary Science Conference. CD-ROM.

Busemann H., Alexander C. M. O'D., and Nittler L. R. 2007. Characterization of insoluble organic matter in primitive meteorites by micro-Raman spectroscopy. *Meteoritics & Planetary Science* 42:1387–1416.

Butenko Y. V., Kuznetsov V. L., Chuvilin A. L., Kolomiichuk V. N., Stankus S. V., Khairulin R. A., and Segall B. 2000. Kinetics of the graphitization of dispersed diamonds at "low" temperatures. *Journal of Applied Physics* 88:4380–4388.

Charon E., Aléon J., and Rouzaud J. N. 2011. Carbons in Acapulco and Lodran at the nanoscale: Comparison with experimental analogs (abstract #5254). 74th Annual Meteoritical Society Meeting. *Meteoritics & Planetary Science* 46.

Christoffersen R. and Buseck P. R. 1983. Epsilon carbide—A low temperature component of interplanetary dust particles. *Science* 222:1327–1329.

Cody G. D. and Alexander C. M. O'D. 2005. NMR studies of chemical structural variation of insoluble organic matter from different carbonaceous chondrite groups. *Geochimica et Cosmochimica Acta* 69:1085–1097.

Cody G. D., Alexander C. M. O'D., Yabuta H., Kilcoyne A. L. D., Araki T., Ade H., Dera P., Fogel M., Militzer B., and Mysen B. O. 2008. Organic thermometry for chondritic parent bodies. *Earth and Planetary Science Letters* 272:446–455.

Croat T. K., Stadermann F. J., Zinner E., and Bernatowicz T. J. 2004. Coordinated isotopic and TEM studies of presolar graphite from Murchison (abstract #1353). 35th Lunar and Planetary Science Conference. CD-ROM.

Dai Z. R., Bradley J. P., Joswiak D. J., Brownlee D. E., Hill H. G. M., and Genge M. J. 2002. Possible in situ formation of meteoritic nanodiamonds in the early solar system. *Nature* 418:157–159.

Daulton T. L., Eisenhour D. D., Bernatowicz T. J., Lewis R. S., and Buseck P. R. 1996. Genesis of presolar diamonds: Comparative high resolution transmission electron microscopy study of meteoritic and terrestrial nano-diamonds. *Geochimica et Cosmochimica Acta* 60:4853–4872.

Daulton T. L., Bernatowicz T. J., Lewis R. S., Messenger S., Stadermann F. J., and Amari S. 2002. Polytype distribution in circumstellar silicon carbide. *Science* 296:1852–1855.

Derenne S., Rouzaud J. N., Clinard C., and Robert F. 2005. Size discontinuity between interstellar and chondritic aromatic structures: A high resolution transmission electron microscopy study. *Geochimica et Cosmochimica Acta* 69:3911.

Derenne S., Rouzaud J. N., Robert F., and Pizzarello S. 2006. Polyaromatic unit from Tagish Lake insoluble organic matter (abstract #1251). 37th Lunar and Planetary Science Conference. CD-ROM.

Deurbergue A., Oberlin A., Oh J. H., and Rouzaud J. N. 1987. Graphitization of Korean anthracites as studied by transmission electron microscopy and X-rays diffraction. *International Journal of Coal Geology* 8:375–393.

Duley W. W. and Grishko V. I. 2001. Evolution of carbon dust in aromatic infrared emission sources: Formation of nanodiamonds. *The Astrophysical Journal* 554: 209–212.

Floss C. and Stadermann F. J. 2009. High abundance of circumstellar and interstellar C-anomalous phases in the primitive CR3 chondrites QUE 99177 and MET 00426. *The Astrophysical Journal* 697:1242–1255.

Galvez A., Herlin-Boime N., Reynaud C., Clinard C., and Rouzaud J.-N. 2002. Carbon nanoparticles from laser pyrolysis. *Carbon* 40:2775–2789.

Gardinier A., Derenne S., Robert F., Behar F., Largeau C., and Maquet J. 2000. Solid state CP/MAS 13C NMR of the insoluble organic matter of the Orgueil and Murchison meteorites: Quantitative study. *Earth and Planetary Science Letters* 184:9–21.

Garvie L. A. J. and Buseck P. R. 2004. Nanosized carbon-rich grains in carbonaceous chondrite meteorite. *Earth and Planetary Science Letters* 224:431–439.

Garvie L. A. J. and Buseck P. R. 2006. Carbonaceous materials in the acid residue from the Orgueil carbonaceous chondrite meteorite. *Meteoritics & Planetary Science* 41:633–642.

Glavin D. P., Callahan M. P., Dworkin J. P., and Elsila J. E. 2011. The effects of parent body processes on amino acids in carbonaceous chondrites. *Meteoritics & Planetary Science* 45:1948–1972.

Guillois O., Ledoux G., and Reynaud C. 1999. Diamond infrared emission bands in circumstellar media. *The Astrophysical Journal* 521:133–136.

Harris P. J. F., Vis R. D., and Heymann D. 2000. Fullerene-like carbon nanostructures in the allende meteorite. *Earth and Planetary Science Letters* 183:355.

Huss R. G. and Lewis S. R. 1994a. Noble gas in presolar diamonds 1: Three distinct component and their applications for diamond origins. *Meteoritics* 29:791–810.

Huss R. G. and Lewis S. R. 1994b. Noble gas in presolar diamonds 2: Component abundances reflect thermal processing. *Meteoritics* 29:811–829.

Huss R. G. and Lewis S. R. 1995. Presolar diamond, SiC, and graphite in primitive chondrites: Abundances as a function of meteorite class and petrologic type. *Geochimica et Cosmochimica Acta* 59:115–160.

Huss R. G., Meshik A. P., Smith J. B., and Hohenberg C. M. 2003. Presolar diamond, silicon carbide, and graphite in carbonaceous chondrites: Implications for thermal processing in the solar nebula. *Geochimica et Cosmochimica Acta* 67:4823.

Jehlicka J. and Rouzaud J. N. 1990. Organic geochemistry of Precambrian shales and schists (Bohemian Massif, Central Europe). *Organic Geochemistry* 16:865–872.

Krot A. N., Zolensky M. E., Wasson J. T., Scott E. R. D., Neil K., and Ohsumi K. 1997. Carbide-magnetite assemblages in type-3 ordinary chondrites. *Geochimica et Cosmochimica Acta* 61:219–237.

Kuznetsov L. V. and Butenko U. V. 2006. Diamond phase transition at nanoscale. In *Ultra nanocrystalline diamond, synthesis, properties and applications*, edited by Shenderova O. A. and Gruen D. M. Norwich, NY; William Andrew Publishing. pp. 405–521.

Le Guillou C. and Brearley A. J. 2010. Distribution of organic matter at the nanoscale in the matrix of MET 00426 (CR3.0) and its relationship with oxysulfides (abstract #5334). 73rd Annual Meteoritical Society Meeting. *Meteoritics & Planetary Science* 45.

Le Guillou C., Rouzaud J. N., Findling N., and Düber S. 2009. Experimental graphitization and oxidation kinetic of nanodiamond: Implication for nebular thermal processing (abstract #2070). 40th Lunar and Planetary Science Conference. CD-ROM.

Le Guillou C., Rouzaud J.-N., Remusat L., Jambon A., and Bourot-Denise M. 2010. Structures, origin and evolution of various carbon phases in the ureilite Northwest Africa 4742 compared with laboratory-shocked graphite. *Geochimica et Cosmochimica Acta* 74:4167–4185.

Le Guillou C., Remusat L., Bernard S., and Brearley A. J. 2011. Redistribution and evolution of organics during aqueous alteration: NanoSIMS-STXM-TEM analyses of FIB sections from Renazzo, Murchison and Orgueil. (abstract #1996). 42nd Lunar and Planetary Science Conference. CD-ROM.

Lewis R. S., Ming T., Wacker J. F., Anders E., and Steel E. 1987. Interstellar diamonds in meteorites. *Nature* 326:160–162.

Lumpkin G. R. 1986. High resolution electron microscopy of carbonaceous materials CI, CM, CV, and H chondrites (abstract). 17th Lunar and Planetary Science Conference. pp. 502–503.

Mostefaoui S., Perron C., Zinner E., and Saïgon G. 2000. Metal-associated carbon in primitive chondrites: Structure, isotopic composition, and origin. *Geochimica et Cosmochimica Acta* 64:1945–1964.

Mostefaoui S., Zinner E., Hopper P., Stadermann F. J., and El Goresy A. 2005. In situ survey of graphite in unequilibrated chondrites: Morphologies, C, N, O, and H isotopic ratios. *Meteoritics & Planetary Science* 40:721–743.

Nakamura K., Zolensky M. E., Tomita S., and Tomeoka K. 2001. In-situ observations of carbonaceous globules in the Tagish Lake meteorite. *Meteoritics & Planetary Science* 36:A145–A146.

Nakamura K., Zolensky M. E., Tomita S., Nakashima S., and Tomeoka K. 2002. Hollow organic globules in the Tagish Lake meteorite as possible products of primitive organic reactions. *International Journal of Astrobiology* 1:179–189.

Nakamura-Messenger K., Messenger S., Keller P. L., Clemet S. J., and Zolensky M. E. 2006. Organic globules in the Tagish Lake meteorite: Remnants of the protosolar disk. *Science* 314:1439–1442.

Oberlin A. 1989. High-resolution TEM studies of carbonization and graphitization. In *Chemistry and physics of carbon*, vol. 22, edited by Thrower P. A. New York: Marcel Dekker. pp. 1.

Oberlin A. and Rouchy J. P. 1971. Transformation des carbones non graphitisables par traitement thermiques en presence de fer. *Carbon* 9:39–46.

Piani L., Robert F., Derenne S., Thomen A., Bourot-Denise M., Mostefaoui S., Marrocchi Y., and Meibom A. 2010. The organic matter in the less metamorphized enstatite chondrite Sahara 97096: Isotopic composition and spatial distribution (abstract #1736). 41st Lunar and Planetary Science Conference. CD-ROM.

Piani L., Robert F., Beyssac O., Binet L., Bourot-Denise M., Derenne S., Le Guillou C., Marrocchi Y., Mostefaoui S., Rouzaud J. N., and Thomen A. 2012. Structure, composition and location of the organic matter in the enstatite chondrite Sahara 97096 (EH3). *Meteoritics & Planetary Science* 47:8–29.

Pizzarello S., Cooper G. W., and Flynn G. J. 2006. The nature and distribution of the organic material in carbonaceous chondrites and interplanetary dust particles. In *Meteorites and the early solar system II*, edited by Lauretta D. S. and McSween H. Y. Tucson, AZ: The University of Arizona Press. pp. 625–651.

Quirico E., Raynal P.-Y., and Bourot-Denise M. 2003. Metamorphic grade of organic matter in six unequilibrated ordinary chondrites. *Meteoritics & Planetary Science* 38:795–811.

Quirico E., Borg J., Raynal P. I., Montagnac G., and D'Hendecourt L. 2005a. A micro-Raman survey of 10 IDPs and 6 carbonaceous chondrites. *Planetary and Space Science* 53:1443–1448.

Quirico E., Rouzaud J. N., Bonal L., and Montagnac G. 2005b. Maturation grade of coals as revealed by Raman spectroscopy. *Spectrochimica Acta Part A* 61:2368–2377.

Quirico E., Montagnac G., Rouzaud J. N., Bonal L., Bourot-Denise M., Duber S., and Reynard B. 2009. Precursor and metamorphic condition effects on Raman spectra of poorly ordered carbonaceous matter in chondrites and coals. *Earth and Planetary Science Letters* 287:185–193.

Quirico E., Bourot-Denise M., Robin C., Montagnac G., and Beck P. 2011. A reappraisal of the metamorphic history of EL3 and EH3 chondrites. *Geochimica et Cosmochimica Acta* 75:3088–3102.

Remusat L., Palhol F., Robert F., Derenne S., and France-Lanord C. 2006. Enrichment of deuterium in insoluble organic matter from primitive meteorites: A solar system origin? *Earth and Planetary Science Letters* 243:15–25.

Remusat L., Le Guillou C., Rouzaud J. N., Binet L., Derenne S., and Robert F. 2008. Molecular study of insoluble organic matter in Kainsaz CO3 carbonaceous chondrite: Comparison with CI and CM IOM. *Meteoritics & Planetary Science* 43:1099–1111.

Remusat L., Robert F., Meibom A., Mostefaoui S., Delpoux O., Binet L., Gourier D., and Derenne S. 2009. Proto-planetary disk chemistry recorded by D-rich organic radicals in carbonaceous chondrites. *The Astrophysical Journal* 698:2087–2092.

Rietmeijer F. J. M. and MacKinnon I. D. R. 1985. Poorly graphitized carbon as a new cosmothermometer for primitive extraterrestrial materials. *Nature* 315:733–736.

Robert F. and Epstein S. 1982. The concentration and isotopic composition of hydrogen, carbon and nitrogen in carbonaceous meteorites. *Geochimica et Cosmochimica Acta* 46:81–95.

Robin C., Quirico E., Bourot-Denise M., and Montagnac G. 2008. Metamorphic grades of enstatite chondrites as revealed by carbonaceous matter (abstract #5224). *Meteoritics & Planetary Science* 43.

Rouzaud J.-N. and Clinard C. 2002. Quantitative high resolution transmission electron microscopy: A promising tool for carbon materials characterization. *Fuel Processing Technology* 77–78:229–235.

Rouzaud J.-N. and Oberlin A. 1989. Structure, microtexture and optical properties of anthracene and saccharose-based carbons. *Carbon* 27:517–529.

Rouzaud J.-N. and Oberlin A. 1990. The characterization of coals and cokes by transmission electron microscopy. In *Advanced methodologies in coal characterization*, edited by Charcosset H. and Nickel-Pepin-Donat B. Amsterdam: Elsevier. pp. 311–355.

Rouzaud J.-N., Skrzypczak A., Bonal L., Derenne S., Quirico E., and Robert F. 2005. The high resolution transmission electron microscopy: A powerful tool for studying the organization of terrestrial and extra-terrestrial carbons (abstract #1322). 36th Lunar and Planetary Science Conference. CD-ROM.

Rubin A. E. and Scott W. R. D. 1997. Abee and related EH chondrite impact-melt breccias. *Geochimica et Cosmochimica Acta* 61:425–435.

Sephton M. A., Pillinger C. T., and Gilmour. 1998. $\delta^{13}C$ of free and macromolecular aromatic structures in the Murchison meteorite. *Geochimica et Cosmochimica Acta* 62:1821–1828.

Smith P. P. K. and Buseck P. R. 1981. Graphitic carbon in the Allende meteorite: A microstructural study. *Science* 212:322–324.

Tomita S., Burian A., Dore J. C., LeBolloch D., Fuji M., and Hayashi S. 2002. Diamond nanoparticles to carbon onions transformation: X-ray diffraction studies. *Carbon* 40:1469–1474.

Van Kerckhoven C., Tielens A. G. G. M., and Waelkens C. 2002. Nanodiamonds around HD97048 and Elias1. *Astronomy and Astrophysics* 384:568–584.

Vis R. D., Mrowiec A., Kooymam P. J., Matsubara K., and Heymann D. 2002. Microscopic search for the carrier phase Q of the trapped planetary noble gases in Allende, Leoville and Vigarano. *Meteoritics & Planetary Science* 37:1391–1399.

Wopenka B. and Pasteris J. D. 1993. Structural characterization of kerogens to granulite-facies graphite: Applicability of Raman microprobe spectroscopy. *American Mineralogist* 78:533–557.

Yang J. and Epstein S. 1983. Interstellar organic matter in meteorites. *Geochimica et Cosmochimica Acta* 47:2199–2216.

Zhai Y., Wan Y., Cheng Y., Shi Y., Zhang F., Tu B., and Zhao D. 2008. The influence of carbon source on the wall structure of ordered mesoporous carbons. *Journal of Porous Materials* 15:601–611.

Zolensky M. E., Bourcier W. L., and Gooding J. L. 1989. Aqueous alteration on the hydrous asteroids: Results of EQ3/6 computer simulations. *Icarus* 78:411–425.

Zolensky M. E., Nakamura K., Gounelle M., Mikouchi T., Kasama T., Tachikawa O., and Tonui E. 2002. Mineralogy of Tagish Lake: An ungrouped type2 carbonaceous chondrites. *Meteoritics & Planetary Science* 37:737–761.